RSC Advances

ROYAL SOCIETY OF CHEMISTRY

www.rsc.org/advances

Binary doped polypyrrole and polypyrrole/boron nitride nanocomposite: preparation, characterization and application in detection of liquefied petroleum gas leaks

Adil Sultan, Sharique Ahmad, Tarique Anwer and Faiz Mohammad*

Department of Applied Chemistry

Faculty of Engineering and Technology

Aligarh Muslim University, Aligarh-202002 (India)

*Corresponding author's email: faizmohammad54@rediffmail.com

Mobile: +919412623533

Abstract

We report the electrical conductivity based rapid response liquefied petroleum gas (LPG) sensor using binary doped polypyrrole and polypyrrole/boron nitride (PPy/BN) nanocomposite as the conductive material. Binary doped PPy and PPy/BN nanocomposite have been synthesized by chemical oxidative *in situ* polymerization method by using $FeCl_3$ as an oxidant in presence of camphorsulfonic acid (CSA). PPy/BN nanocomposite has also been synthesized by chemical oxidative *in situ* polymerization method by using $FeCl_3$ as an oxidant. The PPy/$FeCl_3$/CSA, PPy/BN/$FeCl_3$ and PPy/BN/$FeCl_3$/CSA were characterized using Fourier transform infrared spectroscopy, x-ray diffraction, thermogravimetric analysis and field emission scanning electron microscopy. On the basis of these results, the well-organized structural nanocomposites were successfully prepared owing to the specific interactions between the PPy and the BN nanosheets. Results indicated that the morphology and electrical properties of the nanocomposites were significantly influenced by the BN nanosheets loading and CSA. Transformation of non-conducting PPy/BN/$FeCl_3$ into conducting PPy/BN/$FeCl_3$/CSA was also observed. Addition of CSA caused significant

increment in electrical conductivity due to binary doping of nanocomposites. The as-prepared PPy/$FeCl_3$/CSA and PPy/BN/$FeCl_3$/CSA nanocomposites were studied for the change in their electrical conductivity on exposure to liquefied petroleum gas (LPG) and ambient air at room temperature with the possible use as sensor for detection of LPG leaks.

1. Introduction

Among various applications, conducting polymers have been used as sensors, due to their inherent electronic, optic and mechanical transduction mechanism.[1-8] To enhance sensitivity, considerable efforts have been focused on the fabrication of nanometer scale conducting polymer materials. The beneficial characteristics of these materials include their small dimensions, high surface to volume ratio and amplified sensitivity for sensor-transducer applications.[9-13] Among various morphologies of conducting polymer nanostructures, nanoparticles offer the advantages of small-diameter particles for device fabrication, facile fabrication steps and uniform size and uniform deposition for sensor electrode production without particle aggregation.[14-21]

Among the various conducting polymers, polypyrrole (PPy) is especially promising in commercial applications because of its good environmental stability, facile synthesis and higher conductivity compared with many other conducting polymers. The use of PPy have been demonstrated as biosensors, gas sensors, wires, microactuators, antielectrostatic coatings, solid electrolytic capacitors, electrochromic windows, displays, polymeric batteries, electronic devices, functional membranes and so on.[22-29]

Hexagonal-boron nitride (h-BN) is a layered material consisting of two-dimensional (2D) atomically thin sheets of covalently bonded boron and nitrogen stacked together by weak van der Waals forces. Recently, researchers have been able to exfoliate bulk h-BN materials in large quantities to obtain high surface area h-BN sheets using wet chemical approach and demonstrated its various applications.[30] Hexagonal boron nitride (h-BN) is an analogue of

graphite and has tremendous applications in the fields ranging from optical storage to medical treatment, photocatalysis and electrical insulation due to its wide direct band gap (~5.79 eV) as well as its excellent chemical stability and inoxidizability.[31,32] Recent reports demonstrate lightweight nanocomposites have been prepared by incorporating the thermally conductive nanomaterials such as carbon nanotubes, graphene and boron nitride (BN) nanosheets.[33-39] These individual nanomaterials have ultra-high thermal conductivity due to limited phonon scattering and high phonon velocity. BN is an electrical insulator with a dielectric constant of ~3~4[40] and thus it is widely used in thermal management of high power electronics and display applications that are not possible by using CNTs and graphene.

Conducting polymer composites are of great technical interest as they exhibit a wide range of electrical, optical and magnetic properties. Besides, conducting polymer composites are prepared with various inorganic additives for improving the thermal properties of these materials. Highly fire-resistant materials such as boron phosphate and huntite are also used as additives. **Besides it, Shao et al have also reported the effect of gas exposure on electrical response of CNTs and graphene on account of ease of functionalization at molecular level.[41] Later Saha et al reported that development of CNT networks have a direct influence on the electrical properties and potential applications of composite materials.**[42] Likewise, hexagonal boron nitride (h-BN) is one of the additives used for this purpose.[43,44]

Herein, we present a simple strategy for the preparation of PPy/$FeCl_3$/CSA and PPy/BN/$FeCl_3$/CSA nanocomposites by oxidative polymerization of pyrrole. The effect of the addition of BN nanosheets and binary doping on the physicochemical properties are investigated. The morphology, thermal stability and electrical conductivity of the resulting PPy/$FeCl_3$/CSA and PPy/BN/$FeCl_3$/CSA nanocomposites were also investigated. These surface engineered products were also examined for their dynamic response of electrical

conductivity towards LPG using a simple 4-in-line probe electrical conductivity measurement set up.

2. EXPERIMENTAL

2.1 Materials

Pyrrole 99% (Spectrochem, India), ferric chloride anhydrous (Fisher Scientific, India), boron nitride (MK Nano, Canada), camphorsulfonic acid (TCI, Tokyo) and methanol (E. Merck, India) were used as received. The water used in these experiments was double distilled.

2.2 Synthesis of binary doped PPy and PPy/BN nanocomposites

Pyrrole (0.05 mol) and camphorsulfonic acid (0.01 mol) in 100 mL of distilled water were mixed. A solution of ferric chloride (0.05 mol) in 100 mL distilled water was then poured dropwise into the mixture. The reaction mixture was stirred continuously for about 20 hrs resulting in the formation of black colored solid. The product (PPy/$FeCl_3$/CSA) thus formed was filtered, washed several times with distilled water and methanol and dried in an air oven at 80°C for 6 hrs.

PPy/BN nanocomposites were prepared by oxidative polymerization of pyrrole in the presence of BN nanosheets. In a typical preparation, pyrrole (0.05 mol) and camphorsulfonic acid (0.01 mol) in 100 mL of distilled water were mixed. A uniform suspension of BN (100 mg) in 100 mL deionized water prepared by ultra-sonication for 1 hour was then added into the mixture. A solution of ferric chloride (0.05 mol) in 100 mL distilled water was then poured dropwise into the mixture at room temperature with constant stirring. The colour of the solution changed from greenish to black indicating the polymerization of pyrrole. The resulting solution was then stirred for further 20 hours. The resultant mixture was then filtered, washed thoroughly with distilled water to remove unused reactants and byproducts until the filtrate became colourless. It was further washed thoroughly with methanol to remove any other impurities. The product (PPy/BN/$FeCl_3$/CSA) was dried at 80°C for 6

hours. PPy/BN/$FeCl_3$ was also prepared using same procedure mentioned above without using CSA. The nanocomposite materials were kept in a desicator for further experiments. For electrical conductivity measurements, 0.30 gm material from each sample was pelletized at room temperature with the help of a hydraulic pressure instrument at 100 kN pressure for 15 min.

3. Results and discussion

3.1 Preparation of PPy and PPy/BN nanocomposites

Polypyrrole and polypyrrole/BN nanocomposites were prepared by oxidation of pyrrole in aqueous medium using $FeCl_3$ as an oxidant in presence and absence of CSA. Thus prepared PPy/$FeCl_3$/CSA, PPy/BN/$FeCl_3$ and PPy/BN/$FeCl_3$/CSA were labelled as PPy-2, PPy/BN-1 and PPy/BN-2 respectively where 1 stands for singly doped and 2 stands for binary doped samples as shown in **Figure- 1**.

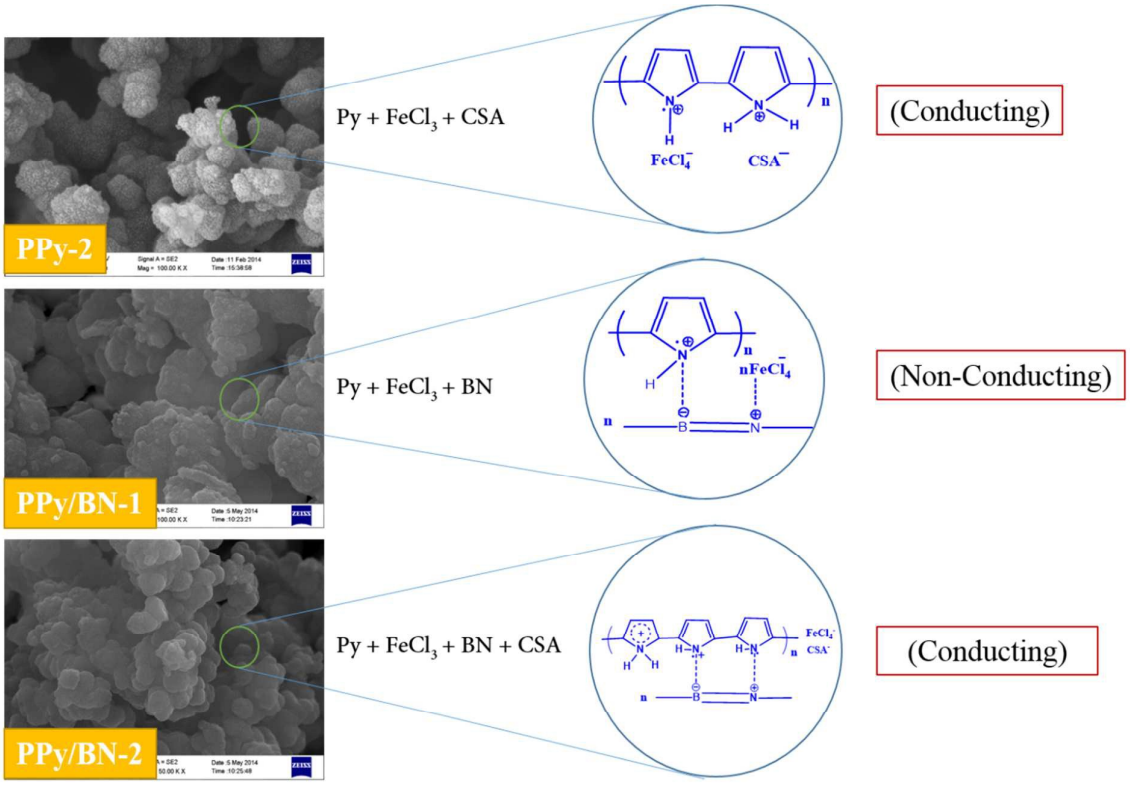

Figure- 1 Schematic presentation of formation of PPy-2, PPy/BN-1 and PPy/BN-2.

3.2 Characterization

The morphology, structure and chemical composition of PPy and PPy/BN nanocomposites were characterized by a variety of techniques including the Fourier transform infrared spectroscopy (FTIR) done using Perkin-Elmer 1725 instrument, X-ray powder diffraction (XRD) and field emission scanning electron microscopy was done by LEO 435–VF. PPy and PPy/BN nanocomposites were studied in terms of their DC electrical conductivity retention under isothermal and cyclic ageing conditions. A four-in-line probe with a temperature controller PID-200 (Scientific Equipment, Roorkee, India) was used to measure the DC electrical conductivity and its temperature dependence. The DC electrical conductivity was calculated by using the following equation:

$$\sigma = \frac{\left[ln2\left(\frac{2S}{W}\right)\right]}{\left[2\pi S\left(\frac{V}{I}\right)\right]} \qquad \textbf{Equation- 1}$$

where I, V, W and S are the current (A), voltage (V), thickness of the pellet (cm) and probe spacing (cm) respectively and σ is the conductivity (Scm^{-1}).[45] In isothermal stability testing, the pellets were heated at 50°C, 70°C, 90°C, 110°C and 130°C and the DC electrical conductivity was measured at an interval of 10 min in the accelerated ageing experiments. In the case of cyclic ageing technique, DC conductivity measurements were taken 5 times at an interval of about 80 min within the temperature range of 40– 150°C. In sensing experiment, two pellets of the each PPy-2 and PPy/BN-2 were tested for LPG sensing property. A cigarette lighter operated by commercially available dry LPG with regulated flow rate of 16.66 ppm/sec was used in the experiment.

3.3 FT-IR spectroscopic study

FT-IR spectra of PPy-2 and PPy/BN nanocomposites were recorded on KBr pellets. The FTIR spectra of PPy-2 shows the main absorption peak at 3429 cm^{-1} corresponding to stretching vibration of N–H bonds as shown in **Figure- 2**. The characteristic absorption bands for C=C, C=N, C-N stretching frequencies were obtained at 1539, 1304 and 1172 cm^{-1}

respectively. In case of PPy/BN nanocomposites the N-H, C=C, C=N and C-N stretching frequencies were observed at 3419, 1558, 1313 and 1192 cm^{-1} respectively. The absorptions bands obtained around 1380 cm^{-1} can be attributed to BN stretching. The slight increase in the N-H, C=C, C=N, C-N stretching frequencies is probably attributed to the interaction of PPy and BN nanosheets. Although stretching frequencies corresponding to NH bonds of PPy were different from that in PPy/BN but their bending frequencies were observed to be a same frequencies and were approximately obtained at 1030 cm^{-1}. The prominent absorption band of CSA was clearly observed at 1633 cm^{-1} which is evidently supporting the formation of PPy-2 and PPy/BN-2 nanocomposites.

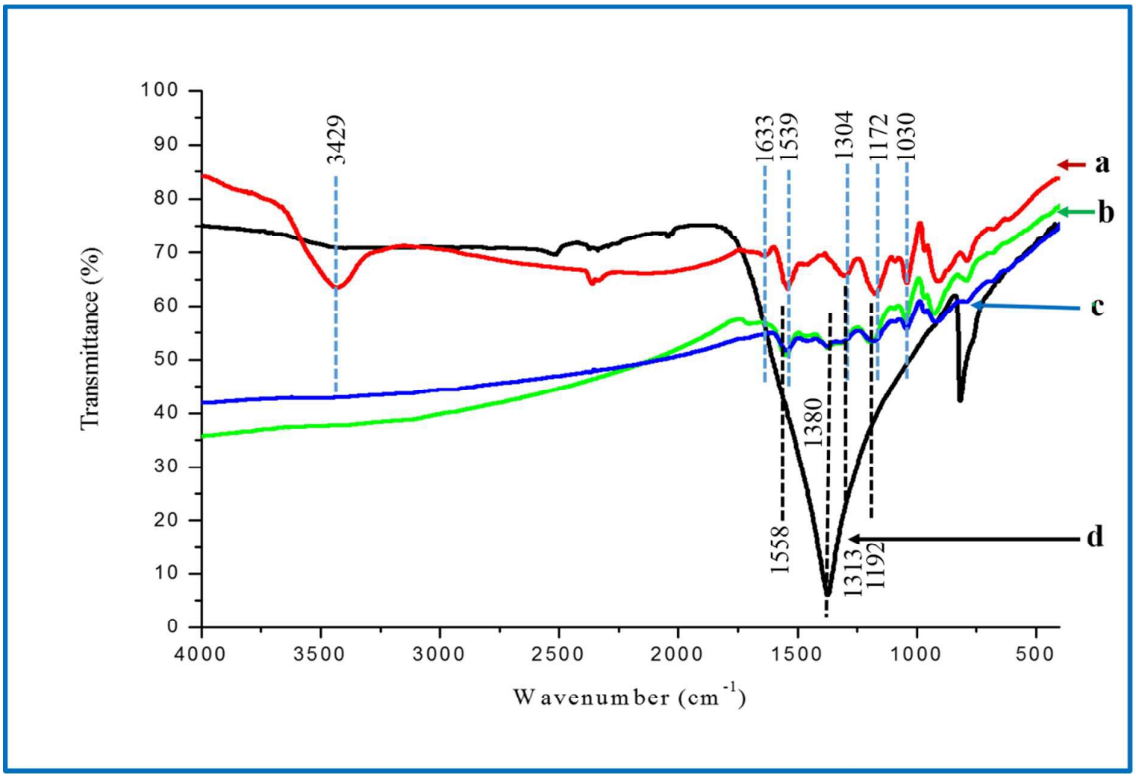

Figure- 2 FT-IR spectra of: (a) PPy-2, (b) PPy/BN-1, (c) PPy/BN-2 and (d) BN.

3.4 X-ray diffraction (XRD) analysis

The crystal structure of the as-prepared PPy-2 and PPy/BN nanocomposites was characterized by XRD. The **Figure- 3 a** shows the spectra of PPy-2, the appearance of broad

peak in the region of 2θ = 26.38° in PPy-2 suggests the presence of polypyrrole. The **Figure-3 b** shows the XRD spectra of PPy/BN-1 nanocomposite. The spectra shows the peaks corresponding to both PPy and BN. The **Figure- 3 c** shows the spectra of PPy/BN-2. The figure shows the peaks relating to PPy and BN which suggests that the structure of the nanocomposite is not altered by the addition of CSA. The broad peak observed at 2θ = 26.26°, suggested that amorphous nature of polypyrrole and crystalline nature of BN has got merged and shifted from 25.66° in the nanocomposite. The **Figure- 3 d** shows that the peaks at 2θ values of 25.66°, 37.10°, 40.83°, 43.55°, 49.24°, 54.23° and 76.81°correspond to the BN.

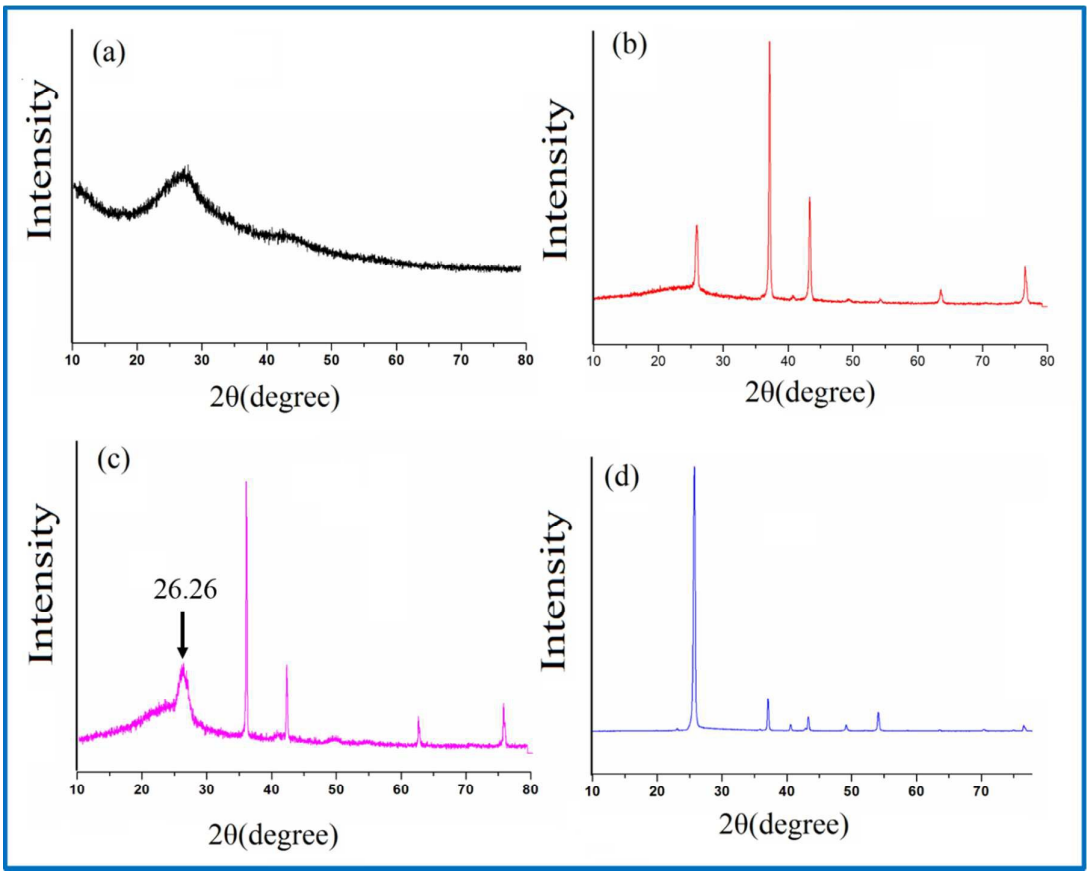

Figure- 3 XRD spectra of: (a) PPy-2, (b) PPy/BN-1, (c) PPy/BN-2 and (d) BN.

3.5 Thermogravimetric Analysis (TGA)

The amount of weight loss and thermal stability of the PPy-2, PPy/BN-1 and PPy /BN-2 nanocomposites were determined by means of TGA in the range of 40- 600°C. From the **Figure- 4**, it may be observed that the degradation process involved the loss of water in PPy and PPy/BN nanocomposites, the elimination of dopant and dedoping process of the polymer. It is clear that decomposition of the PPy-2 started at approximately 191°C, while at 226°C for PPy/BN-2 nanocomposite and all had three weight loss processes. The PPy/BN and PPy/BN-2 nanocomposite show higher thermal stability than that of PPy-2. The shift in decomposition temperature may be related to the interaction between CSA and BN. It is found that in CSA with PPy/BN, a little difference could be observed in thermal stability for nanocomposites but with obvious decrease in the residual weight. The nanocomposites synthesized with and without CSA showed better thermal stability than pure PPy-2, with increased temperature.

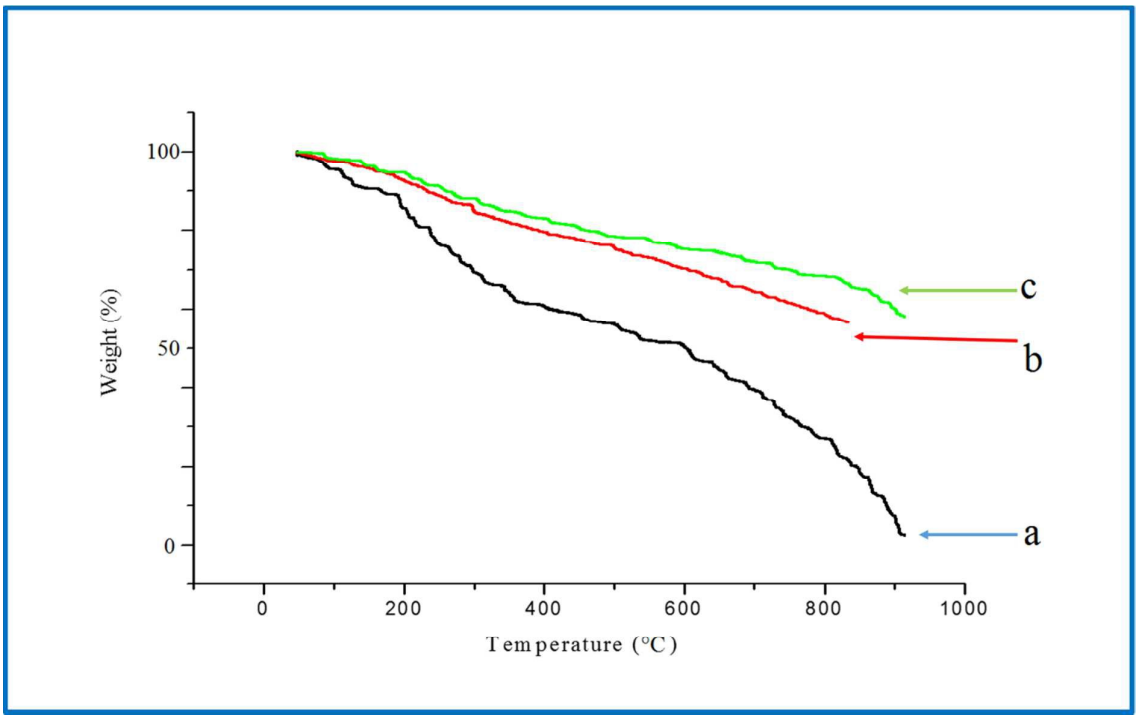

Figure- 4 TGA curve of: (a) PPy-2, (b) PPy/BN-1 and (c) PPy/BN-2

3.6 Scanning electron micrograph studies

The morphology and shape of pure BN, PPy-2, PPy/BN-1 and PPy/BN-2 nanocomposites were characterized by FE-SEM technique and the obtained images are presented in **Figure-5**.

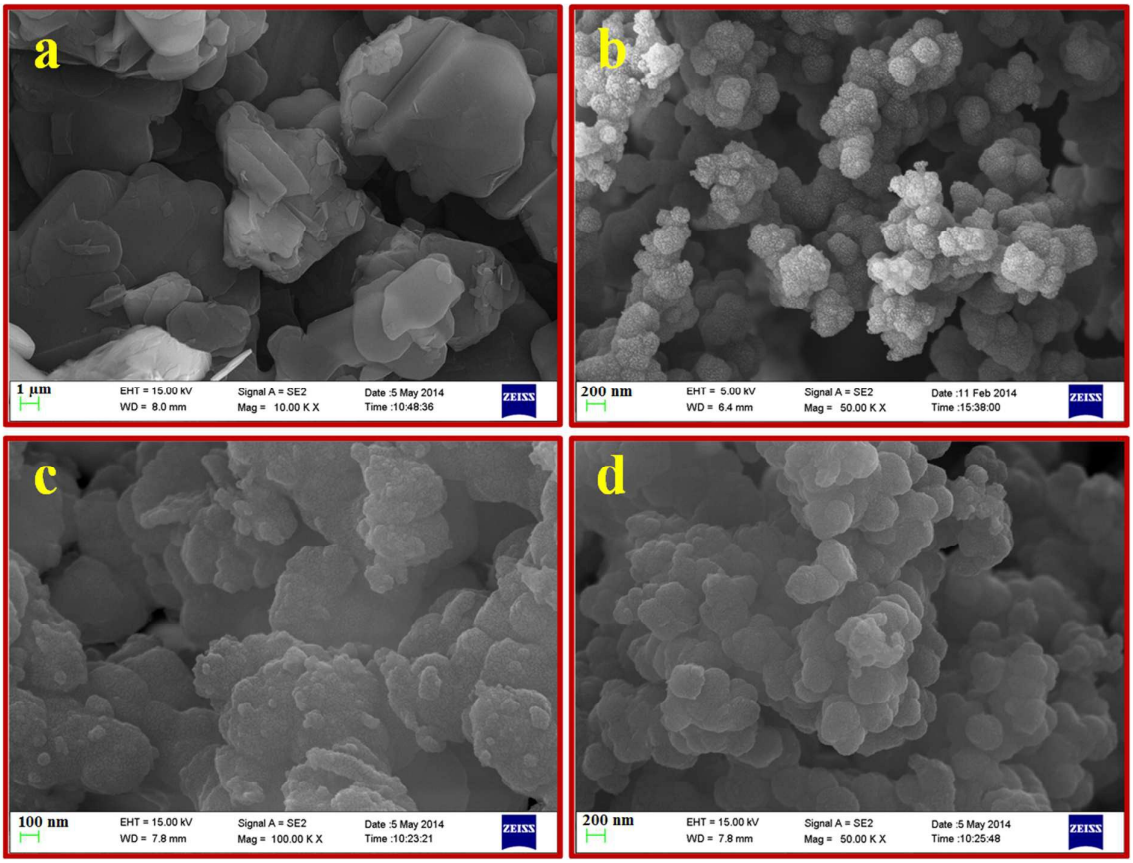

Figure- 5. FE-SEM image of: (a) BN, (b) PPy-2, (c) PPy/BN-1 & (d) PPy/BN-2 nanocomposites showing granular/spherical structures in different magnifications.

The FE-SEM micrograph with high magnification (**Figure- 5 a**) clearly showed nanosheet like structure of h-BN. The FESEM image of PPy-2 nanoparticles is shown in **Figure- 5 b**. It showed that the synthesized polypyrrole is agglomerated by several nanoparticles. The as-prepared PPy/BN-1 is composed of granules approximately 100−200 nm in diameter (**Figure- 5 c**) and the granular structure of PPy is associated with the BN. In **Figure- 5 d** PPy/BN-2 showed the granular/spherical structures associated with CSA. The effect of CSA

on PPy/BN nanocomposite morphology is seen clearly in **Figure- 5 (c & d)**. The nanocomposite prepared with CSA exhibited less compact morphology and seems more regular as evident from **Figure- 5 d** whereas the sample prepared without the surfactant exhibits a very dense and compact structure as shown in F**igure- 5 c**. As the concentration of the incorporated CSA increased, less agglomeration and better dispersion was obtained. The nanocomposites consisting of BN bind to the surface of large PPy polymer granules and their size remains unchanged due to the mild conditions of *in situ* polymerization. The BN is well dispersed in the nanocomposites, and no free BN nanoparticles was present which indicated that the BN nanoparticles and CSA have a nucleating effect on the pyrrole polymerization and caused a homogeneous PPy shell around them.

4. Electrical conductivity

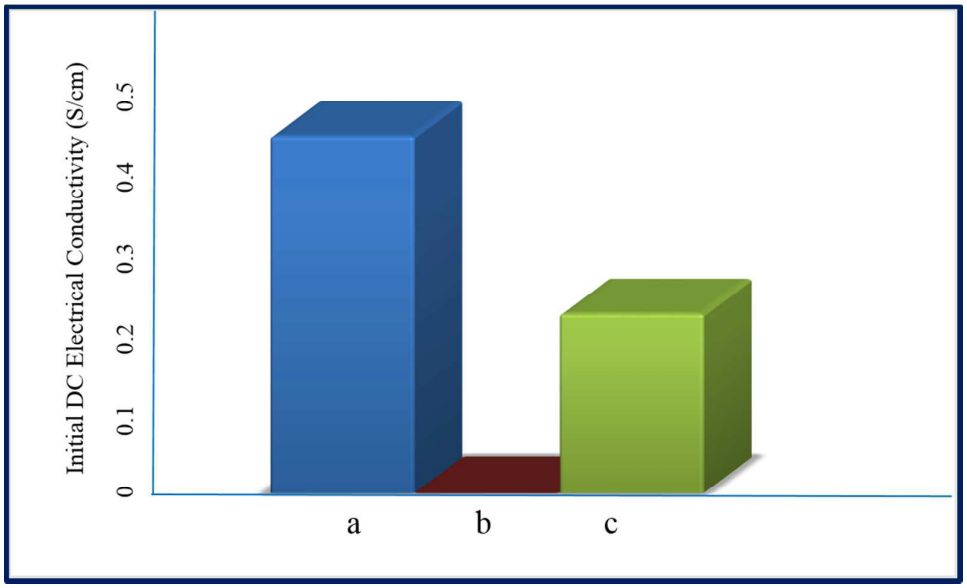

Figure- 6 Initial DC electrical conductivity of: (a) PPy-2, (b) PPy/BN-1 and (c) PPy/BN-2 nanocomposites.

The DC electrical conductivity of PPy-2 and PPy/BN nanocomposites with and without CSA was measured using a 4-in-line probe technique. The electrical conductivity showed decrease

from 0.466 S/cm to 0.234 S/cm after loading boron nitride with CSA but PPy/BN-1 nanocomposites did not show electrical conductivity. In order to complete its octet, B atoms interacts with the lone pair of electrons of N atoms of BN and thus B−N bonds become extremely polar. The highly polar B−N bonds strongly bind the polarons of the PPy and the counterion $FeCl_4^-$ and lock them. This causes the loss of mobility in polarons leading to loss of electrical conductivity in PPy/BN as shown in **Figure- 6**. In CSA doped PPy/BN-2 nanocomposites, the addition of BN increases the compactness of the sample, causing lesser coupling through the grain boundaries which in turn reduces the electrical conductivity. Whereas, in the absence of CSA in PPy/BN-1 nanocomposites, no electrical conductivity was observed which may be due to locking of positive charge on PPy by BN and therefore electrical conductivity is lost due to non-mobile positive charge. With the addition of CSA, a higher crystallinity is obtained which facilitates improvement in charge transfer mechanism and hence, results in increased electrical conductivity.[46] The increase in electrical conductivity may also be due to unlocking of polarons or bipolarons because of interaction of CSA**.** The electrical conductivity is regained as positive charge become mobile as shown in **Figure- 1**.

4.1 Isothermal stability studies

The stability in terms of DC electrical conductivity retention of PPy-2 and PPy/BN-2 nanocomposites was studied under isothermal ageing conditions as shown in **Figure- 7**. The relative electrical conductivity was plotted against time for each temperature as given in the equation below:

$$\sigma_{r,t} = \frac{\sigma_t}{\sigma_\circ}$$ **Equation- 2**

where $\sigma_{r,t}$ = relative electrical conductivity at time t, σ_t = electrical conductivity at time t, σ_o = electrical conductivity at time zero.

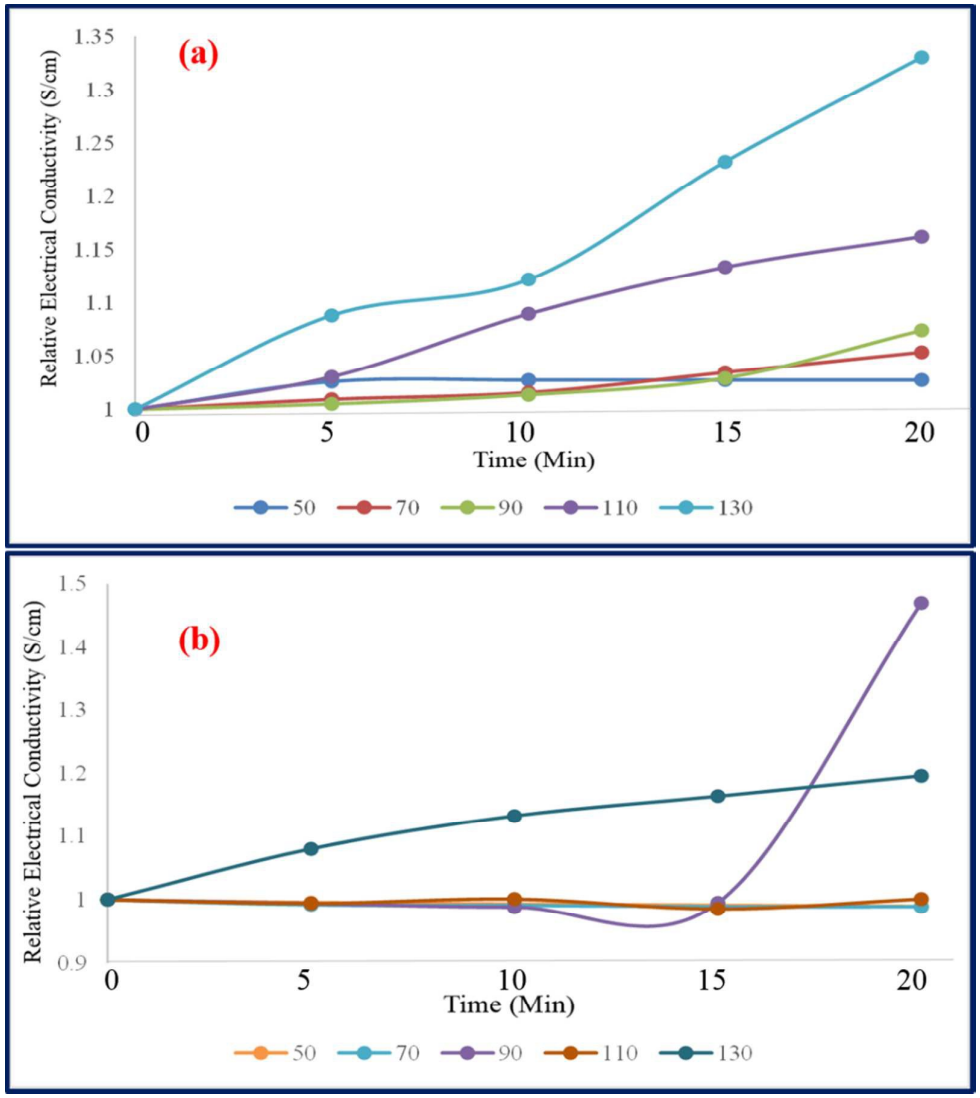

Figure- 7 Change in relative electrical conductivity of: (a) PPy-2 and (b) PPy/BN-2 nanocomposites under isothermal ageing conditions.

The stability in terms of DC electrical conductivity retention of these materials, the best method is to compare the relative electrical conductivity with respect to time at different temperatures for different samples. The DC conductivity of the samples (5 readings of each

sample were taken at an interval of 5 min) was measured at the temperatures 50, 70, 90, 110 and 130°C. **Figure- 7 a** shows that the electrical conductivity of PPy-2 is fairly stable at 50°C, 70°C and 90°C. In case of PPy/BN-2, electrical conductivity is fairly stable at 50°C, 70°C and 110°C as shown in **Figure- 7 b**. The instability shown by PPy/BN-2 at 90°C seems to be due to the instrumental deviation. Thus PPy-2 is observed to be more stable than PPy/BN-2 in the term of electrical conductivity under isothermal aging condition.

4.2 Stability under Cyclic Ageing

The stability in terms of DC electrical conductivity retention of PPy-2, PPy/BN-1 and PPy/BN-2 nanocomposites was also studied by cyclic ageing technique also within the temperature range of 40°C to 130°C as shown in **Figure- 8**. The conductivity measurements were also recorded for subsequent cycles and it was observed that the conductivity decreased gradually from first to fifth cycle showing a regular trend in all the cases. The relative electrical conductivity was calculated using the following equation:

$$\sigma_r = \frac{\sigma_T}{\sigma_{40}} \qquad \textbf{Equation- 3}$$

where σ_r is relative electrical conductivity, σ_T is electrical conductivity at temperature T (°C) and σ_{40} is electrical conductivity at 40°C.

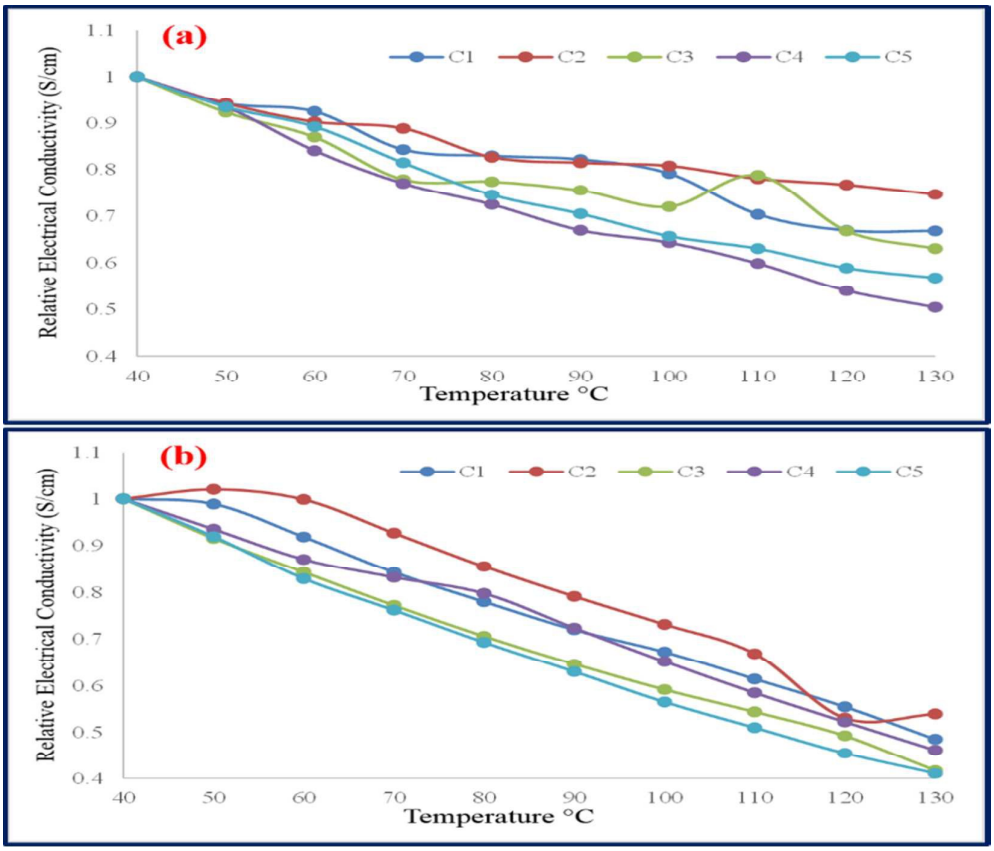

Figure- 8 Relative Electrical conductivity of: (a) PPy-2 and (b) PPy/BN-2 nanocomposites under cyclic ageing conditions.

The decrease in electrical conductivity with the introduction of BN in nanocomposite structure is supposed to be due to the insulating behaviour of boron nitride, because its outer electrons are bound by nitrogen atoms, thus the hindrance in the transport of carriers between different molecular chain of PPy and the interaction at the interface of PPy and boron nitride probably led to the reduction of the conjugation length of PPy in nanocomposites. In case of PPy/BN-2 nanocomposites the electrical conductivity increases due to the doping of CSA due to increase in the number of charge carriers, which can be connected with the delocalization effect of doping and formation of the polarons or bipolarons in the nanocomposite structure, thus enhancing the electrical conductivity of nanocomposites.

4.3 I-V Studies

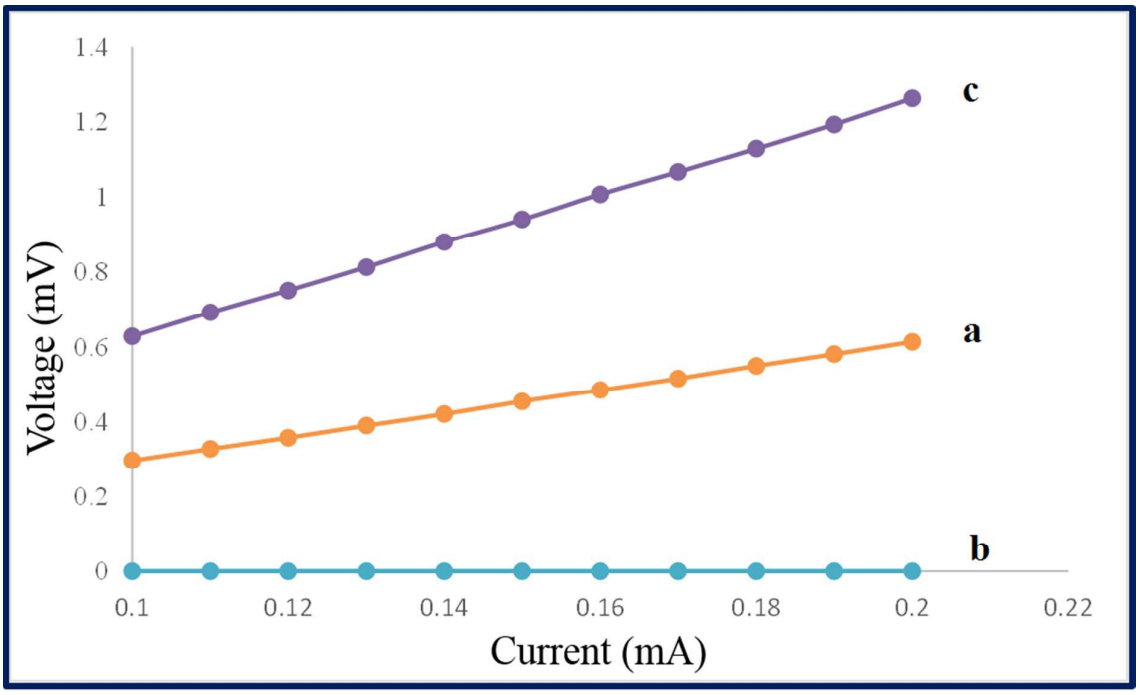

Figure- 9 I-V characteristics of: (a) PPy-2, (b) PPy/BN-1 and (c) PPy/BN-2 nanocomposites.

The current verses voltage plots of the PPy-2, PPy/BN-1 and PPy/BN-2 nanocomposites respectively are shown in **Figure- 9**. The I-V characteristics of these samples were recorded at 80°C. PPy-2 and PPy/BN-2 nanocomposites showed that current increases with increase in voltage while PPy/BN-1 does not show this effect. From the **Figure- 9**, it is observed that the higher electrical conductivity is shown by PPy-2 than that of PPy/BN-2 as electrical conductivity is inversely proportional to voltage. The PPy-2 and PPy/BN-2 showed Ohmic variations which are fairly regular with respect to the applied voltage. This linear increase in current with applied voltage is related to the conduction mechanism of PPy and its nanocomposites. PPy/BN-1 showed I-V behaviour of an insulator.

5. LPG Sensing

Though LPG is known as one of the most common domestic fuels, its leak even at ppm levels may cause irritation and breathing trouble in human beings. LPG is comprised of mainly butane and traces of ethylmercaptan for its characteristic odor that causes irritation and breathing troubles. To study this, we became interested to examine the LPG leaks using the materials prepared in view of –SH groups of ethyl-mercaptan has strong tendency to interact with molecules like PPy and BN at room temperature (~25°C). Source of LPG was a commercial lighter with regulated flow rate and amount of LPG used for sensing study was 2 gm.

Dhawale et al have been synthesized polyaniline/ZnO nanocomposite using electrodepositing polyaniline on chemical bath deposited ZnO film. They explained liquefied petroleum gas (LPG) detection using as prepared nanocomposite and compared with N_2 and CO_2 gases and LPG exhibited maximum response upon exposure of LPG.[47] Later, S. Barkade et al have been synthesized PPy/ZnO nanocomposite using in situ miniemulsion polymerization of pyrrole, which is suitable for liquefied petroleum gas (LPG) sensor development. They observed that the controlled size of hybrid particles using this synthesis strategy minimizes the response time to sense the LPG significantly.[48] However, we have observed the effect of ambient air exposure to the polypyrrole is to decrease the electrical conductivity in our previous work.[49] But herein we have tried to look forward our continued effort and examine the effect of LPG molecules upon electrical conductivity (**Figure- 10**).

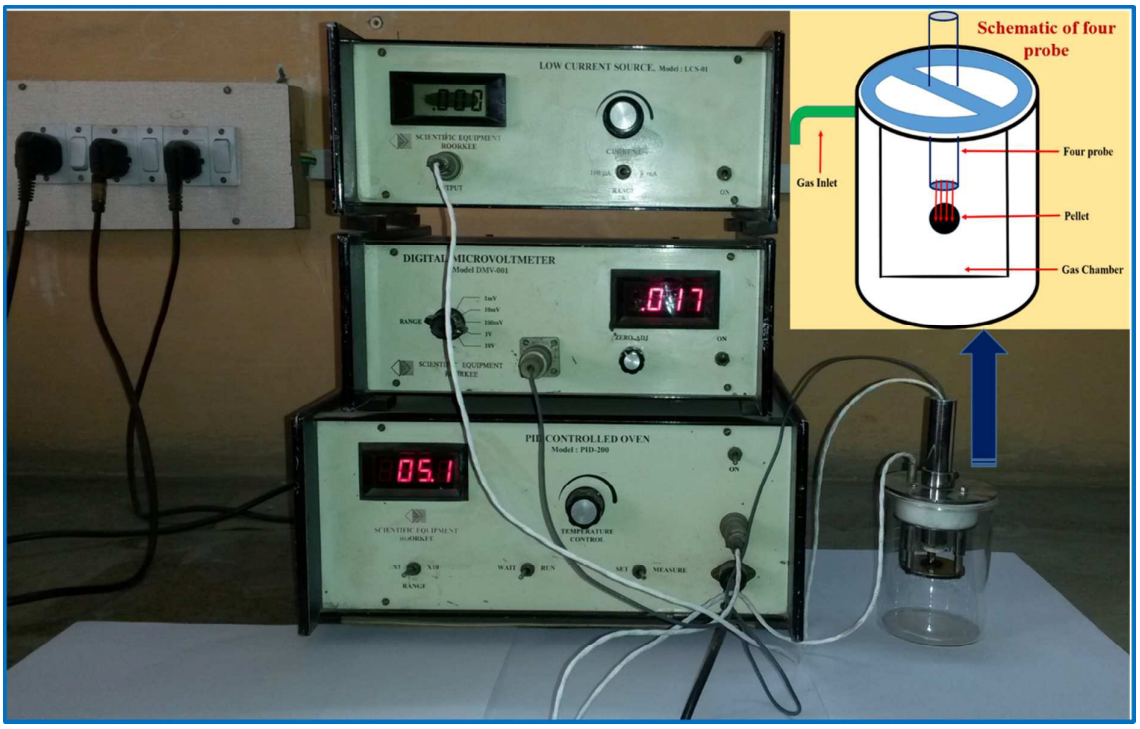

Figure-10 Real set up of gas sensor unit and schematic of four probe measurement unit.

The LPG gas sensitivity of PPy-2 was analysed by measuring the changes in the electrical conductivity at room temperature. The response time and the sensing intensity are the two different factors on which gas sensitivity of PPy-2 was investigated. Gas sensitivity was measured for 60 seconds after which the pellet was exposed to air for further 60 seconds. When PPy-2 was exposed to gas, it was observed that the electrical conductivity decreased with increase in time. The reason for this observed decrease may be due to the nucleophilic property of thiol group of ethylmercaptan, the inherent component of LPG which donates its electron density to electron deficient polypyrrole. This decreases mobility of charge carriers leading to decrease in electrical conductivity. This lowering in charge carriers alongwith decreased delocalization causes drop in electrical conductivity. When the pellet was exposed to air, the electrical conductivity started to increase with time and reached its maximum value after 60 seconds reason being desorption of ethylmercaptan from the surface of PPy-2.

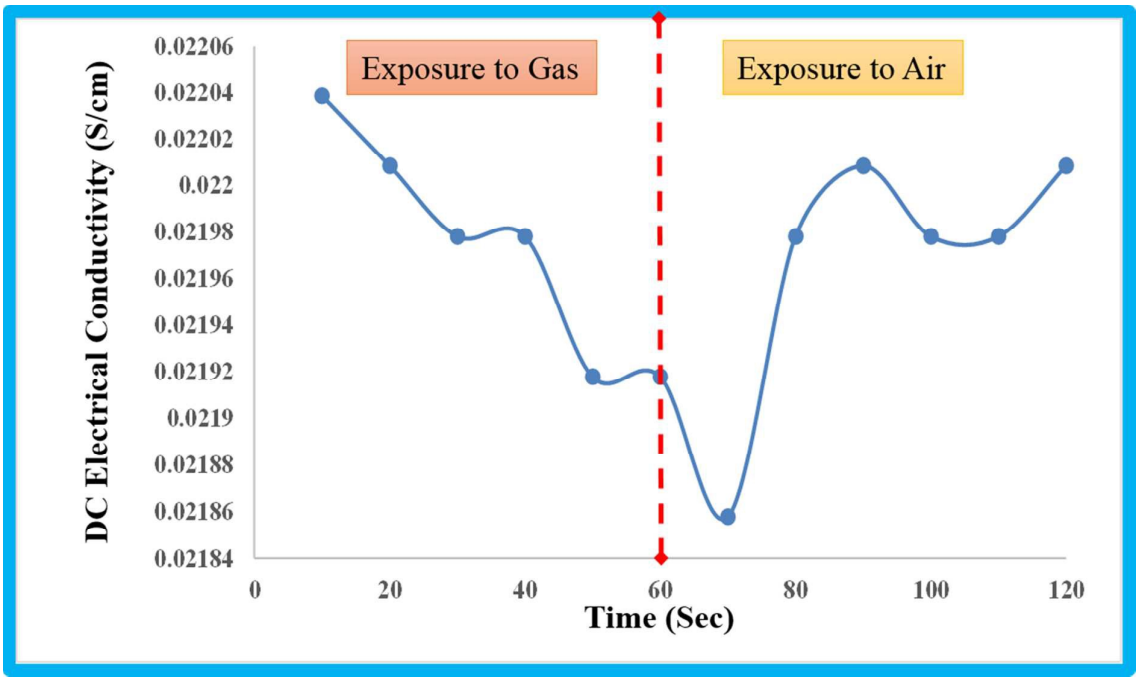

Figure- 11 Effect on the DC electrical conductiviy of PPy-2 on exposure to LPG with respect to time.

The DC electrical conductivity was measured in order to evaluate the reversibility response of PPy-2. This reversibility was measured by first keeping the sample in gas for 10 sec followed by 10 sec in air for a total duration of 120 seconds. As observed from **Figure- 12** the material shows good reversibility.

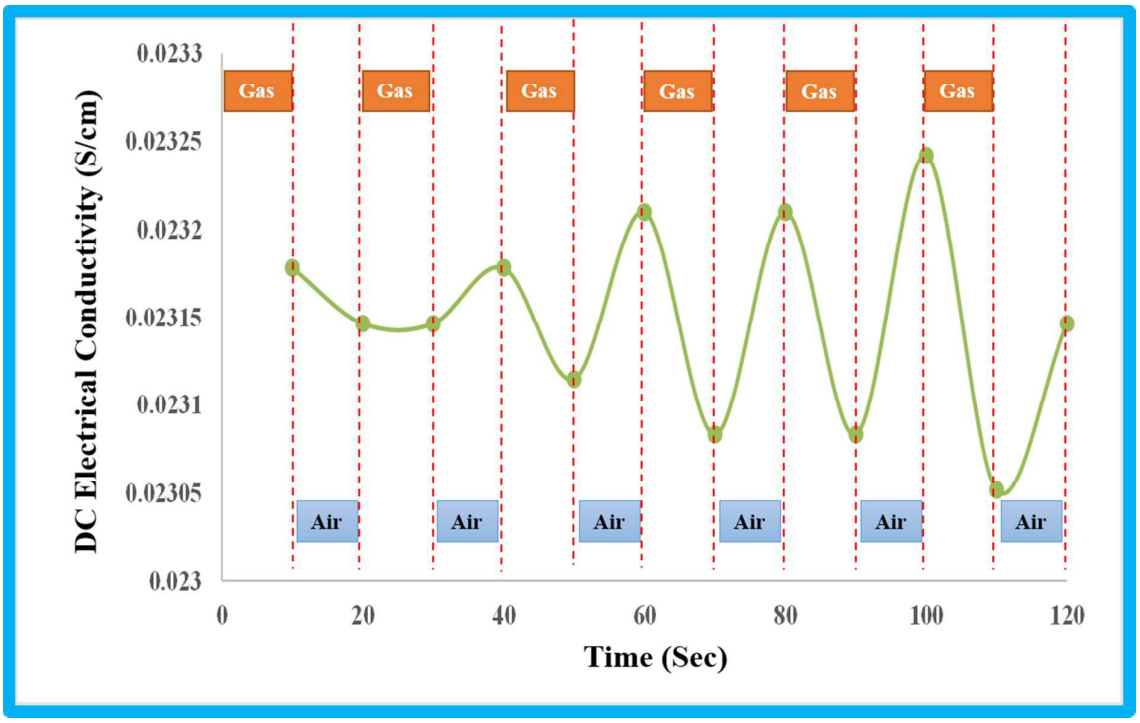

Figure- 12 Variation in electrical conductivity of PPy-2 on alternating exposure to LPG and air.

The gas sensitivity of PPy/BN-2 was analysed by measuring the changes in the electrical conductivity at room temperature. Gas sensitivity was measured for 60 seconds after which the pellet was exposed to air for further 60 seconds. When PPy/BN-2 was exposed to gas, it was observed that the electrical conductivity sharply decreased with increase in time and then levelled off for the reasons mentioned in previous para. When the pellet was exposed to air, the electrical conductivity started to increase with time and then decreased and became constant. It may be suggested that the nanocomposite is composed of two components viz. binary doped PPy and BN salt with CSA. The two components interact with the lone pair of ethyl-mercaptan differently i.e. reversible interaction with binary doped polypyrrole and irreversible interaction with BN salt with CSA.

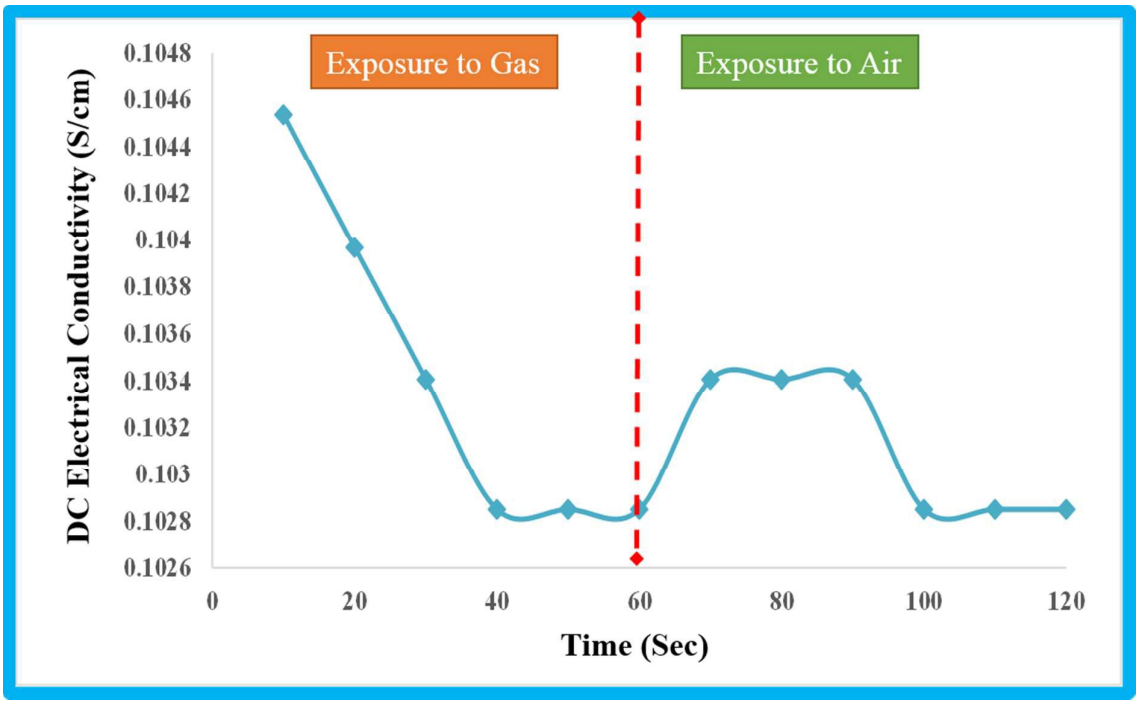

Figure- 13 Effect on the electrical conductiviy of PPy/BN-2 on exposure to LPG with respect to time.

The DC electrical conductivity of PPy/BN-2 composite was also measured in order to evaluate the reproducibility response as it was done in previous case. The reproducibility was measured by first keeping the sample in gas for 10 sec followed by 10 sec in air for a total of 120 seconds. It may be observed from **Figure- 14** that the nanocomposite showed poor reversibility than PPy-2, which confers that there occurs no desorption of gas molecules from the surface.

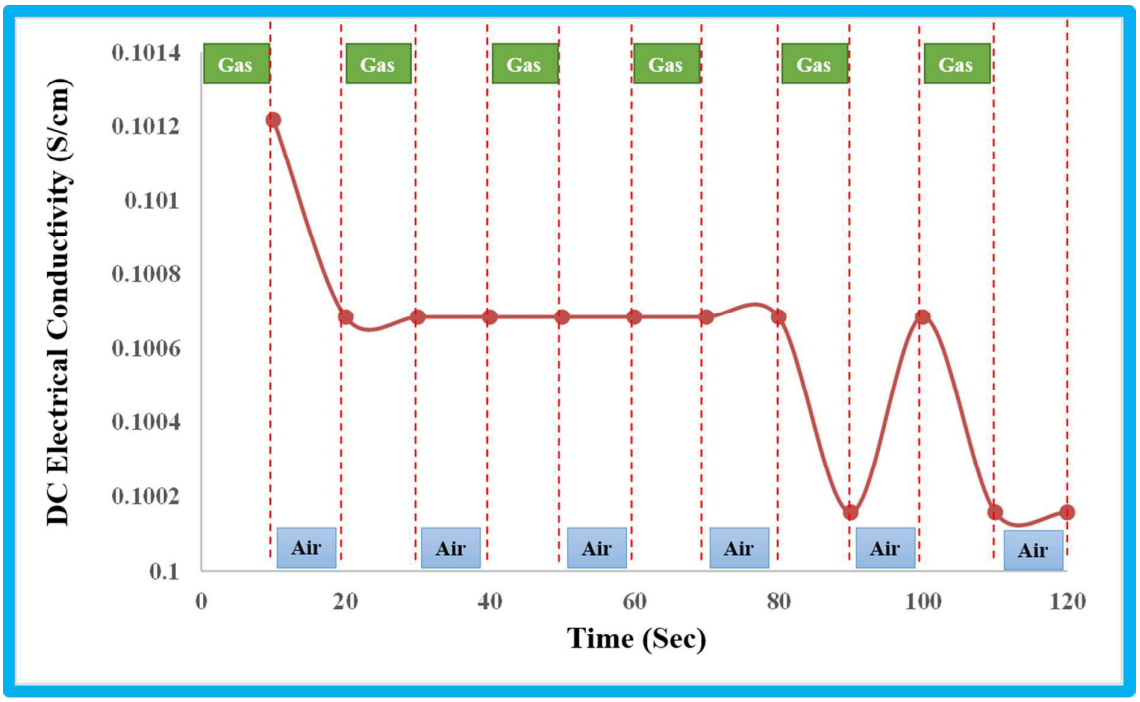

Figure- 14 Variation in conductivity of PPy/BN-2 on alternating exposure to LPG and air.

5.1 Proposed Mechanism for LPG sensing:

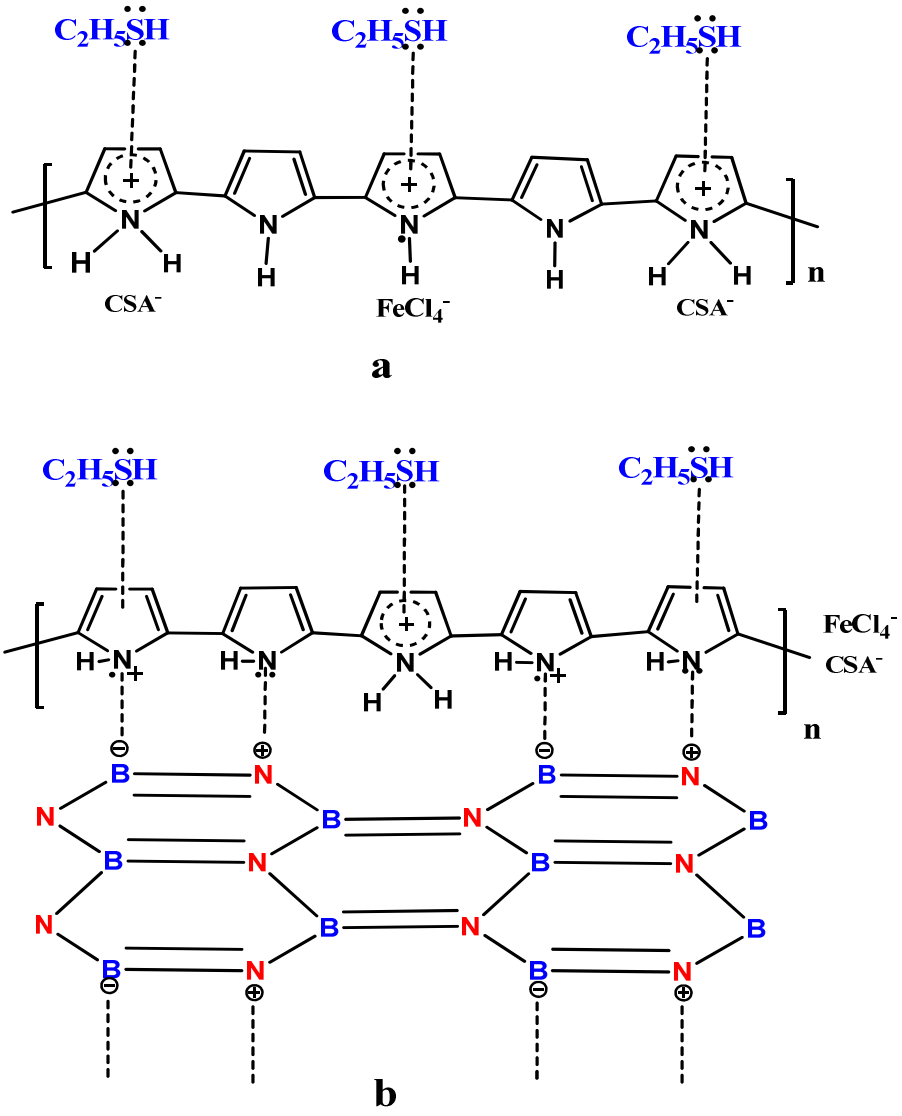

Scheme- 1 Proposed interaction between LPG gas and (a) PPy-2, (b) PPy/BN-2.

The sensing mechanism of LPG gas was explained on the basis of adsorption and desorption process through the DC electrical conductivity at room temperature. A variation occurs in the DC electrical conductivity after exposure to LPG. As the PPy-2 is exposed to LPG, the electrical conductivity decreases. The decrease in electrical conductivity is attributed to the decrease in charge carriers as the LPG molecules reach the surface of PPy-2. When the pellet is then exposed to air, the electrical conductivity again reaches the starting value. In case of

PPy/BN-2 nanocomposite, the DC electrical conductivity decreases after exposure to LPG and remains almost same after exposure to air. The change in DC electrical conductivity may be due to physico-chemical adsorption between nanocomposite and absorbed gas molecules.

The chemical composition of LPG is butane, propane, traces of ethyl mercaptan and other hydrocarbons. At room temperature only ethyl mercaptan is reactive, butane, propane and other hydrocarbons do not react. In case of PPy-2, the ethyl mercaptan is adsorbed on the surface via interaction between lone pairs of sulfur and polaron of the polypyrrole ring. This interaction leads to localization of polypyrrole ring electrons which in turn causes the decrease in mobility of charge carriers thereby decreasing electrical conductivity.

In case of PPy/BN-2 nanocomposite, the lone pairs of nitrogen and polarons of polypyrrole ring interact with electron deficient nitrogen and negatively charged boron atoms of boron nitride ring, respectively. As the LPG gas interacts with this nanocomposite, the lone pairs of sulfur atom of ethyl mercaptan bind strongly with polarons of the polypyrrole ring, which decreases the electrical conductivity. After the composite is exposed to air the irreversible nature of conductivity is observed because of the strong interaction of ethyl mercaptan with polarons of the polypyrrole ring.

Conclusion

The PPy/BN nanocomposite with and without CSA was successfully synthesized by in-situ polymerization method. FTIR and XRD analysis confirmed the presence of BN and PPy. FESEM analysis shows uniform dispersion of the BN in the polypyrrole and effect of CSA clearly seen. The DC electrical conductivity observed with the addition of CSA in PPy/BN nanocomposite. The results highlighted that this material can be applied in gas sensing field to develop LPG sensors with performances for practical application. Therefore, the sensor based on PPy/BN-2 may be useful for single shot investigations i.e. as dosimeter.

Acknowledgment. Adil Sultan gratefully acknowledge Mr. Nayeem Ahmed for helpful discussions.

References

1. C. Basavaraja, Y. M. Choi, H. T. Park, D. S. Huh, J. W. Lee, M. Revanasiddappa, S. C. Raghavendra, S. Khasim and T. K. Vishnuvardhan, Bull. Korean Chem. Soc. 2007, **28**, 1104.
2. T. K. Vishnuvardhan, V. R. Kulkarni, C. Basavaraja and S. C. Raghavendra, Bull. Mater. Sci. 2006, **29**, 77.
3. H. S. Song, O. S. Kwon, S. H. Lee, S. J. Park, U. K. Kim, J. Jang and T. H. Park, Nano Lett. 2013, **13**, 172–178.
4. S. Cho, O. S. Kwon, S. A. You and J. Jang, J. Mater. Chem. A 2013, **1**, 5679–5688.
5. O. S. Kwon, S. J. Park, J. S. Lee, E. Park, T. Kim, H. W. Park, S. A. You, H. Yoon and J. Jang, Nano Lett. 2012, **12**, 2797–2802.
6. S. H. Lee, O. S. Kwon, H. S. Song, S. J. Park, J. H. Sung, J. Jang and T. H. Park, Biomaterials 2012, **33**, 1722–1729.
7. H. Yoon, S. H. Lee, O. S. Kwon, H. S. Song, E. H. Oh, T. H. Park and J. Jang, Angew. Chem., Int. Ed. 2009, **48**, 2755–2758.
8. O. S. Kwon, S. J. Park, H. Yoon and J. Jang, Chem. Commun. 2012, **48**, 10526–10528.
9. S. H. Choi, G. Ankonina, D. Y. Youn, S. G. Oh, J. M. Hong, A. Rothschild and I. D. Kim, ACS Nano 2009, **3**, 2623–2631.
10. O. Landau, A. Rothchild and E. Zussman, Chem. Mater. 2009, **21**, 9–11.

11. O. S. Kwon, S. J. Park, H. W. Park, T. Kim, M. Kang, J. Jang and H. Yoon, Chem. Mater. 2012, **24**, 4088–4092.

12. H. Yoon and J. Jang, Adv. Funct. Mater. 2009, **19**, 1567–1576.

13. H. Yoon, M. Chang and J. Jang, Adv. Funct. Mater. 2007, **17**, 431–436.

14. J. Jang, Adv. Polym. Sci. 2006, **199**, 189–259.

15. D. T. McQuade, A. E. Pullen and T. M. Swager, Chem. Rev. 2000, **100**, 2537–2574.

16. J. Jang, J. H. Oh and G. D. Stucky, Angew. Chem., Int. Ed. 2002, **41**, 4016–4019.

17. O. S. Kwon, S. R. Ahn, S. J. Park, H. S. Song, S. H. Lee, J. S. Lee, J. Y. Hong, J. S. Lee, S. A. You and H. Yoon, ACS Nano 2012, **6**, 5549–5558.

18. O. S. Kwon, J. H. Hong, S. J. Park, Y. Jang and J. Jang, J. Phys. Chem. C 2010, **114**, 11874–18879.

19. D. Zhai, B. Liu, Y. S. Pan, Y. Wang, W. Li, R. Zhang and G. Yu, ACS Nano 2013, **7**, 3540–3546.

20. S. Radhakrishnan, C. Sumathi, A. Umar, S. J. Kim, J. Wilson and V. Dharuman, Biosens. Bioelectron. 2013, **47**, 133–140.

21. M. Xu, J. Z. Wang, X. Guo, H. Xia, Y. Wang, S. Zhang, W. Huang and S. Wu, Sens. Actuators, B 2010, **146**, 8–13.

22. J. C. Vidal, E. Garcia and J. R. Castillo, Anal. Chim. Acta 1999, **385**,213.

23. T. E. Campbell, A. J. Hodgson and G. G. Wallace, *Electroanalysis* 1999, **11**, 215.

24. D. Kincal, A. Kamer, A. D. Child and J. R. Reynold, Synth. Met. 1998, **92**, 53.

25. N. T. Kemp, G. U. Flanagan, A. B. Kaiser, H. J. Trodahl, B. Chapman, A. C. artridge and R. G. Buckley, Synth. Met. 1999, **101**, 434.

26. C. Jerome, D. Labaye, I. Bodart and R. Jerome, Synth. Met. 1999, **101**, 3.

27. E. J. Smela, Micromech. Microeng. 1999, **9**, 1.

28. M. Selvaraj, S. Palraj, K. Maruthan, G. Rajagopal and G. Venkatachari, Synth. Met. 2008, **158**, 888.

29. J. Li, L. Zhu, B. Shu and H. Tang, Synth. Met. 2008, **158**, 516.

30. J. T. Tijerina, T. N. Narayanan, G. Gao, M. Rohde, D. Tsentalovich, M. Pasquali and P. M. Ajayan, ACS Nano 2012, **6**, 1214−1220.

31. K. Watanabe, T. Taniguchi and H. Kanda, Nat. Mater., 2004, **3**, 404.

32. Y. Kubota, K. Watanabe, O. Tsuda and T. Taniguchi, Science, 2007, **317**, 932.

33. C.W. Nan, G. Liu, Y. Lin and M. Li, Appl. Phys. Lett. 2004, **85**, 3549-3551.

34. L. Kumari, T. Zhang, G. H. Du, W. Z. Li, Q. W. Wang, A. Datye and K. H. Wu, Compos. Sci. Technol. 2008, **68**, 2178-2183.

35. Z. Han and A. Fina, A review. Prog. Polym. Sci. 2011, **36**, 914-944.

36. X. L. Wang, H. Bai, Z. Y. Yao, A. R. Liu and G. Q. Shi, J. Mater. Chem. 2010, **20**, 9032- 9036.

37. S. H. Song, K. H. Park, B. H. Kim, Y. W. Choi, G. H. Jun, D. J. Lee, B. S. Kong, K. W. Paik and S. Jeon, Adv. Mater. 2013, **25**, 732-737.

38. J. U. Lee, D. Yoon, H. Kim, S. W. Lee and H. Cheong, Phys. Rev. B 2011, **83**, 081419.

39. W. L. Song, P. Wang, L. Cao, A. Anderson, M. J. Meziani, A. J. Farr, Sun and Y. P. Angew. Chem., Int. Ed. 2012, **51**, 6498-6501.

40. C. R. Dean, A. F. Young, MericI, C. Lee, L. Wang, S. Sorgenfrei, K. Watanabe, T. K. P. Taniguchi, K. L. Shepard and J. HoneNat Nano 2010, **5**, 722-726.

41. Y. Shao, J. Wang, H. Wu, J. Liu, I. A. Aksay and Y. Lina, Electroanalysis 2010, **22**, 1027 – 1036.

42. A. Saha, C. Jiang and A. A. Martí, Carbon, 2014, **79**, 1-18.

43. A. Lipp, K. A. Schwetz and K. Hunold, J Eur Ceram Soc 1989, **5**, 3.

44. F. S¸en, and M. V. Kahraman, Prog Org Coat 2014, **77**, 1053.

45. M. O. Ansari, S. K. Yadav, J. W. Cho and F. Mohammad, Composites Part B 2013, **47**, 155.

46. S. G. Pawar, S. L. Patil, M. A. Chougule, B. T. Raut, P. R. Godase, R. N. Mulik, S. Sen and V. B. Patil, 2011, IEEE Sensor J, **11**, 2980–2985.

47. D.S. Dhawale, D.P. Dubal, A.M. More, T.P. Gujar and C.D. Lokhande, Sensors and Actuators B 2010, **147**, 488–494.

48. S. S. Barkade, D. V. Pinjari, A. K. Singh, P. R. Gogate, J. B. Naik, S. H. Sonawane, M. A. kumar and A. B. Pandit, Ind. Eng. Chem. Res. 2013, **52**, 7704−7712.

49. F. Mohammad, J. Phys. D: Appl. Phys. **31**, 1998, 951-959.